# Determination of the parameters of a color neutral 3D color glass condensate model

Şener Özönder

Phys. Rev. D **87**, 045013 — Published 14 February 2013

DOI: 10.1103/PhysRevD.87.045013

# Determination of the Parameters of a Color Neutral 3D Color Glass Condensate Model

Şener Özönder*

*School of Physics and Astronomy, University of Minnesota, Minneapolis, Minnesota 55455, USA*

We consider a version of the McLerran-Venugopalan model by Lam and Mahlon where confinement is implemented via colored noise in the infrared. This model does not assume an infinite momentum frame nor that the boosted nuclei are infinitely thin; rather, nuclei have a finite extension in the longitudinal direction and therefore depend on the longitudinal coordinate. In this fully three dimensional framework an x dependence of the gluon distribution function emerges naturally. In order to fix the parameters of the model, we calculate the gluon distribution function and compare it with the JR09 parametrization of the data. We explore the parameter space of the model to attain a working framework that can be used to calculate the initial conditions in heavy ion collisions.

* ozonder@umn.edu

## I. INTRODUCTION

In heavy ion collisions at very high energies, soft (small-x) partons, mostly gluons, constitute a big portion of the wave function of the colliding nuclei. Since the occupation number of the gluons is very high, they can be treated in the framework of classical Yang-Mills theory. When two nuclei pass through each other, the classical nonabelian fields from each nucleus interact with each other and form color flux tubes between the receding nuclei, which ultimately lead to the quark gluon plasma. The energy density distribution of the initial state determines the multiplicity and spectrum of the final particles seen in the detectors. The initial energy density distribution is an input to the hydrodynamics description of the evolving quark gluon plasma and, in principle, it can be calculated ab initio from Quantum Chromodynamics (QCD).

The energy initially deposited in the color flux tubes can be related to the two-point vector potential correlation function $\langle A_i^a(\boldsymbol{x})A_i^b(\boldsymbol{x}')\rangle$ where the setup may be two (transverse) or three dimensional, depending on whether or not the Lorentz contracted nucleus is assumed to have a longitudinal thickness in the lab frame. This correlator can be derived analytically from the color charge density correlator $\langle\rho^a(\boldsymbol{x})\rho^b(\boldsymbol{x}')\rangle$ by using the classical Yang-Mills equations.

The color charge density of a nucleus $\rho^a(\boldsymbol{x})$ during a collision cannot be known; on the other hand, the fluctuations in the color charge density can be studied in the effective field theory approach with ensemble averaging. In the Color Glass Condensate (CGC), a framework for slowly evolving high density gluons within the ultrarelativistic nucleus, the fast partons are seen as sources of the small-x (soft) gluon radiation, where x is the fraction of the total longitudinal momentum carried by a parton. After integrating out the fast partons, the observables can be calculated by averaging them over the ensemble of all possible color charge configurations. Once the correlator $\langle\rho^a(\boldsymbol{x})\rho^b(\boldsymbol{x}')\rangle$ is specified, it can be linked to the vector field correlator $\langle A_i^a(\boldsymbol{x})A_i^b(\boldsymbol{x}')\rangle$ from which the gluon distribution function $xg(x,Q^2)$ and other observables, such as the initial energy density, can be calculated. Here $\langle\cdots\rangle$ denotes the ensemble average. See Ref. [1] for a comprehensive review.

In the early formulation of the CGC by McLerran and Venugopalan [2–6], the spectrum of the Gaussian color fluctuations was taken to be white noise. This results in arbitrarily long wavelength fluctuations where $\langle A_i^a(\boldsymbol{x})A_i^b(\boldsymbol{x}')\rangle$ diverges in the infrared. This problem

originates from the fact that confinement effects (color neutrality) have not been taken into account. Adding a gluon mass to the gluon propagator so as to bypass this problem breaks gauge invariance which is required later to convert the solution of the classical Yang-Mills equations from the axial gauge to the light-cone gauge by means of Wilson lines.

In the original McLerran-Venugopalan (MV) model, the colliding nuclei are considered to be two-dimensional infinitely thin sheets traveling at the speed of light. In this approximation, the model does not depend on the longitidunal coordinate, hence there is no dependence on the momentum fraction x of a given parton. In other words, all of the partons in the nucleus have the same momentum fraction x. Being an artifact of the infinite momentum frame, the lack of x dependence in the model does not reflect the true nature of the x dependent gluon distribution functions.

In this paper, we consider a color neutral three dimensional McLerran-Venugopalan (3dMVn) model by Lam and Mahlon [7, 8], where the spectrum of the Gaussian fluctuations is taken to be infrared-safe colored noise. Colored noise creates a correlation hole in the correlation function on the size of a nucleon and this leads to color neutrality. (The term "colored noise" is not related to the color charge of QCD.) This model comes with another important feature that the incoming nuclei are not exactly on the light cone. Longitudinal coordinate dependence produces an x dependent gluon distribution function. This enables us to compare the model with the data parametrization of gluon distribution functions and therefore fix the parameters of the 3dMVn model. Once this is achieved, the 3dMVn model can be used to calculate the initial energy density distribution in heavy ion collisions.

The MV model provides a framework for calculating the vector field correlation function $\langle A_i^a(\boldsymbol{x}) A_i^b(\boldsymbol{x}')\rangle$ from which the gluon distribution function as well as the initial energy density distribution can be calculated. We emphasize that our ultimate goal is calculating the latter, which will be pursued in a follow-up paper. In this paper we focus on the calculation of gluon distribution function and its comparison with data for the purpose of fixing the free parameters in the 3dMVn model.

The outline of the paper is as follows. First, we give a brief overview of the color neutral x dependent McLerran-Venugopalan (3dMVn) model given by Lam and Mahlon [7, 8]. Next, we calculate the gluon distribution function from the 3dMVn model. This model works at low-$Q^2$ where no data for the gluon distribution functions is available. For that reason, we evolve our results with the DGLAP equation to higher momenta where data is available.

This is followed by a discussion of the data parametrization that we use to compare with the 3dMVn model. Lastly, we compare the 3dMVn with the data parametrization. The final section summarizes our analysis and includes a discussion regarding how the results will be used in the future to calculate initial energy density distribution.

## II. COLOR NEUTRALITY

In the original two dimensional MV model, the average and the fluctuations of the color charge density of a nucleus are given by

$$\langle \rho^a(\boldsymbol{x}_\perp)\rangle = 0, \tag{1}$$

$$\langle \rho^a(\boldsymbol{x}_\perp)\rho^b(\boldsymbol{x}'_\perp)\rangle = \delta^{ab}\mu_A^2\,\mathcal{D}(\boldsymbol{x}_\perp - \boldsymbol{x}'_\perp), \tag{2}$$

where $\boldsymbol{x}_\perp$ is the transverse coordinate system for the infinitely thin nucleus, $\mu_A^2$ is the average color charge density squared per unit (transverse) area for a nucleus, and $\langle\cdots\rangle$ denotes the ensemble average. The function $\mathcal{D}$ determines the spectrum of the fluctuations. When white noise is assumed, $\mathcal{D}(\boldsymbol{x}_\perp - \boldsymbol{x}'_\perp) = \delta^2(\boldsymbol{x}_\perp - \boldsymbol{x}'_\perp)$, no correlation occurs between different points in a nucleus. This also means that fluctuations in each momentum mode, including the zero mode, are equally likely and there is no characteristic scale. In this case, even though the correlator $\langle A_i^a(\boldsymbol{x}_\perp)A_i^b(\boldsymbol{x}'_\perp)\rangle$ is calculated with an infrared cutoff $\Lambda_{\mathrm{QCD}}$ [9], it still diverges like $(\boldsymbol{x}_\perp^2)^{\boldsymbol{x}_\perp^2}$ in the infrared. Therefore, the Fourier transform of it, which is necessary to calculate the gluon distribution function, does not exist [7]. This cut-off can also be understood as a gluon mass in the gluon propagator in the form $(\boldsymbol{q}_\perp^2 + m_{\mathrm{gluon}}^2)^{-1}$. It explicitly breaks the gauge invariance that is needed to convert the solutions of classical Yang-Mills equations from the axial gauge to the light-cone gauge where Wilson lines are to be used.

In reality, a nucleus is color neutral on scales larger than a nucleon size. A color neutral correlation function can be derived from a simple model of a nucleus where nucleons are composed of quark and antiquark pairs [10]. If we consider a two dimensional nucleus for a moment, the assumption that only the quark and antiquark pair from the same nucleon can interact with each other produces a correlator of the form [7]

$$\langle \rho^a(\boldsymbol{x}_\perp)\rho^b(\boldsymbol{x}'_\perp)\rangle = \delta^{ab}\mu_A^2\left[\delta^2(\boldsymbol{x}_\perp - \boldsymbol{x}'_\perp) - \frac{\exp\left[-|\boldsymbol{x}_\perp - \boldsymbol{x}'_\perp|^2/4\lambda^2\right]}{4\pi\lambda^2}\right]. \tag{3}$$

Here the parameter $\lambda$, which we will refer to as a correlation length, is of the order of a nucleon size $\sim 1\,\mathrm{fm}$. This parameter takes away the need for a sharp infrared cutoff as it is

used in the original MV treatment; moreover, it makes the Fourier transform of the vector field correlation function well-defined and it renders the model infrared safe. In Eq. (3), decorrelation due to the white noise $\mathcal{D}(\boldsymbol{x}_\perp - \boldsymbol{x}'_\perp) = \delta^2(\boldsymbol{x}_\perp - \boldsymbol{x}'_\perp)$ is modified by the last term for distances $|\boldsymbol{x}_\perp - \boldsymbol{x}'_\perp| \lesssim \lambda$, reflecting the assumption that there is a correlation between the partons confined to a region smaller than the nucleon size. The second part in Eq. (3) removes the zero mode $|\boldsymbol{q}_\perp| = 0$ from the white noise spectrum, hence colored noise. The Fourier transform of the correlator in Eq. (3) is proportional to $1 - e^{-\lambda^2 \boldsymbol{q}_\perp^2}$, which vanishes as $|\boldsymbol{q}_\perp| \to 0$. This makes the model infrared safe.

In this paper, we adopt a three dimensional correlator given by Lam and Mahlon [8]

$$\langle \rho^a(0,0)\rho^b(\boldsymbol{x})\rangle = \delta^{ab}\kappa_A^3 \left[\delta^3(\boldsymbol{x}) - \frac{3}{4\pi\lambda^2}\frac{\exp\left(-\sqrt{3}|\boldsymbol{x}|/\lambda\right)}{|\boldsymbol{x}|}\right]. \tag{4}$$

where $\kappa_A^3$ is the three dimensional average color charge density

$$\kappa_A^3 = \frac{3AC_F}{N_c^2 - 1}\frac{1}{V} = \frac{3A}{2N_c}\frac{1}{V}, \tag{5}$$

Here $N_c$ is the number of colors, $V$ is the volume of a nucleus and the color factor is defined as $C_F = (N_c^2 - 1)/(2N_c)$. We define $d^3\boldsymbol{x} \equiv dx_\parallel d^2\boldsymbol{x}_\perp$ where $x_\parallel$ is the longitudinal coordinate in the direction of the beam axis, and $\boldsymbol{x}_\perp$ is the coordinate on the transverse plane. The Fourier transform of the corralator (4) is given by

$$\widetilde{\langle \rho^a \rho^b\rangle} = \delta^{ab}\kappa_A^3 \left[1 - \frac{1}{1 + \lambda^2\boldsymbol{q}^2/3}\right]. \tag{6}$$

Despite the slight difference between the correlators in Eqs. (3) and (4), they produce similar results. It can be readily seen from Eq. (6) that the zero mode does not exist in the spectrum since $\widetilde{\langle \rho^a \rho^b\rangle} \to 0$ as $|\boldsymbol{q}| \to 0$.

## III. LONGITUDINAL DEPENDENCE

In ultrarelativistic heavy ion collisions, the infinite momentum frame provides a good starting point for the parton picture of the nucleus. However, the nucleus becomes infinitely thin when it is exactly on the light cone and the gluon distribution function turns out to be independent of x. Here we review the formulation by Lam and Mahlon [8] for the case where the nucleus is boosted to speed $\beta$. In the lab frame, the thickness a nucleus of radius $R$ becomes of the order of $R/\gamma$.

The current for a nucleus moving in the $+z$ direction is

$$J_r^0 = \rho(-z, \boldsymbol{x}_{\perp r}); \quad \boldsymbol{J}_r = 0, \tag{7}$$

where the subscript "r" stands for the rest frame and the negative sign in front of the $z$ is for later convenience. With the redefinition $x^{\pm} = -x_{\mp} = (t \pm z)/\sqrt{2}$, the current can be rewritten in the light-cone coordinates (still in the rest frame),

$$J_r^+ = J_r^- = \frac{1}{\sqrt{2}}\rho\left(\frac{1}{\sqrt{2}}(x_r^- - x_r^+), \boldsymbol{x}_{\perp r}\right); \quad \boldsymbol{J}_{\perp r} = 0. \tag{8}$$

When we go from the rest frame to the lab frame where the nucleus moves with speed $\beta$, the current in Eq. (8) becomes

$$J^+ = \frac{1}{\varepsilon}\rho\left(\frac{1}{\varepsilon}x^- - \frac{\varepsilon}{2}x^+, \boldsymbol{x}_{\perp}\right); \quad J^- = \frac{\varepsilon}{2}J^+; \quad \boldsymbol{J}_{\perp} = 0, \tag{9}$$

where

$$\varepsilon = \sqrt{\frac{2(1-\beta)}{1+\beta}}. \tag{10}$$

Here we can define a new longitudinal coordinate

$$x_{\parallel} \equiv \frac{1}{\varepsilon}x^- - \frac{\varepsilon}{2}x^+, \tag{11}$$

which is essentially the Lorentz tranformation of $-z = (x^- - x^+)/\sqrt{2}$ (see the definition below Eq. (7)). The Eq. (9) can be contrasted with the commonly used current in the infinite momentum frame (imf) where the nucleus is infinitely thin,

$$J_{\rm imf}^+ = \delta(x^-)\rho(\boldsymbol{x}_{\perp}); \quad J_{\rm imf}^- = 0; \quad \boldsymbol{J}_{\perp \rm imf} = 0. \tag{12}$$

## IV. CALCULATION AND EVOLUTION OF THE GLUON DISTRIBUTION FUNCTION

We now turn to the calculation of the gluon distribution function from the 3dMVn model. Later we will compare it with data in order to fix the parameters $\alpha_s$ and $\lambda$. The gluon distribution function of a nucleus with a baryon number $A$ can be expressed as an integral of the gluon number density over the transverse momenta,

$$g_A(x, Q^2) \equiv \int_{|\boldsymbol{q}_{\perp}| \leqslant Q} d^2\boldsymbol{q}_{\perp} \frac{dN}{dx d^2\boldsymbol{q}_{\perp}}. \tag{13}$$

The gluon number density in the lab frame for a nucleus moving with speed $\beta$ is given as a Fourier transform of the two-point vector field correlation function [8]

$$\frac{dN}{dq_\parallel d^2\boldsymbol{q}_\perp} \equiv \frac{q_\parallel}{4\pi^3}\int d^3\boldsymbol{x}\int d^3\boldsymbol{x}\,' e^{i\boldsymbol{q}\cdot(\boldsymbol{x}-\boldsymbol{x}\,')}\langle A_i^a(\boldsymbol{x})A_i^a(\boldsymbol{x}\,')\rangle, \tag{14}$$

Here $q_\parallel$ is the momentum conjugate to the coordinate defined in Eq. (11). The Eq. (14) can be related to $dN/dxd^2\boldsymbol{q}_\perp$ by using the relation $x \equiv q_\parallel/m$, which itself can be derived from the definition $x \equiv q^+/Q^+ = \varepsilon q^+/m$. Here $m$ is the nucleon mass, $q^+$ and $Q^+$ are the momenta of the gluon and the nucleon.

Solving the classical Yang-Mills equations for the source in Eq. (8) in the covariant gauge and transforming the solution into the light-cone gauge by using Wilson lines, one can express the correlator $\langle A_i^a(\boldsymbol{x})A_i^a(\boldsymbol{x}\,')\rangle$ in Eq. (14) in terms of the color charge density correlator $\langle \rho^a(\boldsymbol{x})\rho^a(\boldsymbol{x}\,')\rangle$. We skip the details of this calculation here and refer the reader to the original paper [8]. Using the correlator in Eq. (4), the gluon number density can be written as

$$\frac{dN}{dxd^2\boldsymbol{q}_\perp} = \frac{2A\alpha_s}{\pi^2}\frac{1}{x}\int d^2\boldsymbol{\Delta}_\perp e^{i\boldsymbol{q}_\perp\cdot\boldsymbol{\Delta}_\perp}\mathcal{L}(x;\boldsymbol{\Delta}_\perp)\mathcal{E}(v^2L(\boldsymbol{\Delta}_\perp)), \tag{15}$$

Here the integration is over the transverse coordinate $\boldsymbol{\Delta}_\perp = \boldsymbol{x}_\perp - \boldsymbol{x}'_\perp$. The functions $\mathcal{L}$ and $L$ are convolutions of the two gluon propagators at two different points in the same nucleus connected by the three dimensional noise term $\mathcal{D}(\boldsymbol{x}-\boldsymbol{x}\,')$. These two functions can be seen as a pair distribution function. The nuclear correction factor $\mathcal{E}$ takes into account the nuclear geometry and $v^2$ controls the strength of dependence on this geometry.

The functions used in Eq. (15) are given as [8]

$$\mathcal{L}(x;\boldsymbol{\Delta}_\perp) = -\frac{1}{12\pi}(xm\lambda)^2K_0(xm\Delta_\perp), \tag{16}$$

and

$$L(\boldsymbol{\Delta}_\perp) = -\frac{\lambda^2}{6\pi}\left[K_0\left(\frac{\sqrt{3}\Delta_\perp}{\lambda}\right) + \ln\left(\frac{\sqrt{3}\Delta_\perp}{2\lambda}\right) + \gamma_{\rm E}\right], \tag{17}$$

where $\Delta_\perp = |\boldsymbol{\Delta}_\perp|$. In the calculations of Lam and Mahlon [8], the nuclear matter density is taken to be uniform. The nuclear correction factor $\mathcal{E}$ is determined by geometry of the nucleus. For cylindrical and spherical nuclei it is given by

$$\mathcal{E}(z) = \begin{cases} \dfrac{1}{z}(e^z-1) & \text{(cylindrical)}, \\ \\ \dfrac{3}{z^3}[1-\dfrac{1}{2}z^2+e^z(z-1)] & \text{(spherical)}. \end{cases} \tag{18}$$

This function appears in Eq. (15) as $\mathcal{E}(v^2 L(\Delta_\perp))$. The $v^2$ controls how much the results depend on the nuclear geometry; it is given by

$$v^2 = \begin{cases} \dfrac{3Ag^4}{2\pi R^2} \approx 24\pi\alpha_s^2 A^{1/3} R_0^{-2} & \text{(cylindrical)}, \\ \\ \dfrac{9Ag^4}{4\pi R^2} \approx 36\pi\alpha_s^2 A^{1/3} R_0^{-2} & \text{(spherical)}. \end{cases} \tag{19}$$

Here $R = R_0 A^{1/3}$ and we take $R_0 = 1\,\text{fm}$. The difference between the spherical and cylindrical nuclei is negligibly small. In our calculations, we use the formulae for a cylindrical nucleus.

Now we are ready to calculate the gluon distribution function $xg_A(x, Q^2)$ for a nucleus by substituting Eq. (15) in Eq. (13),

$$xg_A(x, Q^2) = \frac{2A\alpha_s}{\pi^2} \int_{|\boldsymbol{q}_\perp| \leqslant Q} d^2\boldsymbol{q}_\perp \int d^2\boldsymbol{\Delta}_\perp e^{i\boldsymbol{q}_\perp \cdot \boldsymbol{\Delta}_\perp} \mathcal{L}(x; \boldsymbol{\Delta}_\perp) \mathcal{E}(v^2 L(\boldsymbol{\Delta}_\perp)). \tag{20}$$

The momentum integration in the equation above is trivial. Owing to the longitudinal coordinate $x_\parallel$, the fractional momentum distribution function $xg_A(x, Q^2)$ in Eq. (20) is x dependent, in contrast to the results of the original two dimensional MV model.

The region of validity of the 3dMVn model within the two dimensional parameter space $(x, Q^2)$, likewise the original MV model, is restricted by the assumptions made regarding the weak coupling limit, color coherence and color averaging [8].

The lower limit of x is set for a gold nucleus by

$$x \sim \frac{A^{-1/3}}{mR_0} \simeq 0.035 \tag{21}$$

where $R_0$ is the nucleon size $\sim 1\,\text{fm}$. This is the longitudinal momentum fraction at which the gluons start to resolve the Lorentz contracted thickness of the nucleus.

The weak coupling limit imposes an upper limit on x such that

$$x \lesssim \frac{4}{\pi m R_0} \simeq 0.25. \tag{22}$$

For very large $Q^2$, not enough color charge would be seen, hence the Gaussian approximation for the color charge fluctuations $\langle \rho^a(\boldsymbol{x}) \rho^b(\boldsymbol{x}') \rangle$ would not be valid. Similarly, at the scale of color neutral nucleons where $Q^2$ is very small, again there would not be enough color charge to average over. These considerations put limits on the momentum scale

$$\frac{\pi m}{4R_0} x \lesssim Q^2 \lesssim \frac{4}{m R_0^3} \frac{1}{x}. \tag{23}$$

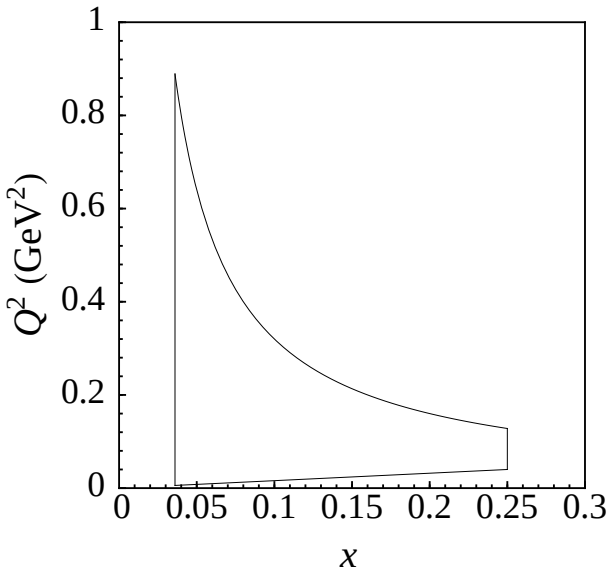


FIG. 1. Approximate region of validity of the 3dMVn model for gold nucleus (A=197).

For $R_0 = 1\,\mathrm{fm}$, Eq. (23) becomes

$$0.16\,x \lesssim Q^2 \lesssim \frac{0.032}{x}. \tag{24}$$

In our calculations, we will take $Q^2 = 0.55\,\mathrm{GeV}^2$. The reason for this choice is that it is at the upper limit of validity of the 3dMVn model and at the lower limit of the parton distribution function to which we will compare. While the model spans a larger range in x for $Q^2 < 0.55\,\mathrm{GeV}^2$ (see Figure 1), no data is available at those scales. At the energy scale $Q^2 = 0.55\,\mathrm{GeV}^2$, x is restricted to the range

$$0.035 < x < 0.060. \tag{25}$$

Figure 1 shows the approximate validity region of the 3dMVn model for a gold nucleus. We consider gold because it provides for the greatest range of validity of the model as represented by Eq. (21). The results for lead would be indistinguishable.

The parameters of the 3dMVn model need to be fixed before performing the numerical integration in Eq. (20). We take the nucleon mass $m = 0.94\,\mathrm{GeV}$, $R_0 = 1\,\mathrm{fm}$ and $A = 197$. The coupling constant $\alpha_s$ and the correlation length $\lambda$ are treated as free parameters. We evaluate $xg_A(x, Q^2)$ numerically at $Q^2 = 0.55\,\mathrm{GeV}^2$ in the range $0.035 < x < 0.060$ for

several values of $\alpha_s$ and $\lambda$ in increments of 0.1 in the range

$$\begin{aligned} 0.1 \leq & \alpha_s \leq 1, \\ 0.2\,\mathrm{fm} \leq & \lambda \leq 2.6\,\mathrm{fm}. \end{aligned} \tag{26}$$

Then we fit $xg_A(x,Q^2)$ to a form

$$xg_A(x,Q^2) = b\,x^c\,(1-x)^d, \tag{27}$$

and find $\{b,c,d\}$ for each set of $\{\alpha_s,\lambda\}$. After the numerical integration, we obtain $xg_{197}(x,Q^2)$ for the whole nucleus for several points in the parameter space $\{\alpha_S,\lambda\}$. The scale $Q^2 = 0.55\,\mathrm{GeV}^2$ at which we calculated $xg_A(x,Q^2)$ is the lower limit of the JR09 data parametrization for the parton distribution functions. For this reason, we will evolve the gluon distribution functions evaluated at $Q^2 = 0.55\,\mathrm{GeV}^2$ to higher momentum values such as $Q^2 = 25$, 100 and $1000\,\mathrm{GeV}^2$ and compare them with data at those scales.

Gluon distribution functions are evolved to different energy scales with the DGLAP equation [11–14]. For this purpose, we employ the code QCDNUM17 [15]. We will assume that nucleus is a dilute system of nucleons and take the nuclear modification factor $R_A = 1$ [16]. Hence,

$$xg_{p/A}(x,Q^2) \equiv \frac{1}{A} xg_A(x,Q^2), \tag{28}$$

where the subscript $p/A$ refers to a nucleon in a nuclear environment. Henceforth, we will use the gluon distribution function for a single nucleon in a gold nucleus. It should be kept in mind that $g_{p/A}(x,Q^2)$ is in principle different than a gluon distribution function for an isolated proton $g_p(x,Q^2)$ since the nuclear effects introduce enhancement or shadowing depending on the energy scale $Q^2$.

We run QCDNUM in the variable-flavor number scheme (vfns) and at the NNLO($\overline{\mathrm{MS}}$) order. For the DGLAP evolution of the gluons, valence and sea quark distributions at the initial scale should also be provided to the evolution code. At the initial scale $Q^2 = 0.55\,\mathrm{GeV}^2$, the calculated gluon distribution function is the main input to QCDNUM. As for the valence and sea quark distributions, the JR09 [17] data parametrization is utilized. The evolution is repeated for several values of $\alpha_s$ and $\lambda$ in the range given in Eq. (26).

## V. DATA PARAMETRIZATION

We will compare our results with the parametrization of data by JR09 [17]. We use the pdfs that work in the vfns scheme and at the NNLO($\overline{\text{MS}}$) order. The JR09 is valid in the ranges

$$\begin{aligned} 0.55 \lesssim & Q^2 \lesssim 10^8\,\text{GeV}^2, \\ 10^{-9} \lesssim & x \lesssim 1. \end{aligned} \tag{29}$$

The JR09 provides pdfs for separate nucleons $xg_p(x,Q^2)$ but it does not contain any information about the nuclear modification function $R_A$. Our results, on the other hand, are for a nucleon in a nuclear environment $xg_{p/A}(x,Q^2)$; therefore, $R_A$ should be, in principle, taken into account. However, the nuclear pdfs (for example nCTEQ [18]) are available only for $Q^2 > 1\,\text{GeV}^2$. As pointed out earlier, since the DGLAP equation mixes quarks and gluons during the evolution, we need the valence and sea quark distribution functions at the initial energy scale so that the gluon distribution function calculated from the model can be evolved to the higher energies. Hence, for consistency, we will utilize the quark pdfs provided by JR09 at $Q^2 = 0.55\,\text{GeV}^2$ as an input to the DGLAP evolution. The discrepancy between JR09 and nCTEQ [18], encoded in the nuclear modification factor, is at most 5% at $Q^2 = 25\,\text{GeV}^2$. At $Q^2 = 100$ and $1000\,\text{GeV}^2$ the discrepancy is negligibly small. For that reason, we think the lack of information regarding $R_A$ will not cause a significant error in our analysis.

## VI. BEST FIT PARAMETERS

Now we seek the sets of parameters $\{\alpha_s, \lambda\}$ that produce the best fits. For this reason, we compare the gluon distribution functions, calculated and evolved to $Q^2 = 100\,\text{GeV}^2$, with JR09 at the same energy.

In the DGLAP evolution to higher energies, the contribution to the radiation at a particular value of x always comes from the sources from the larger x region. Hence, the effect of gluons calculated from 3dMVn in the range $0.035 < x < 0.060$ at $Q^2 = 0.55\,\text{GeV}^2$ will be more prominent at smaller x values at $Q^2 = 100\,\text{GeV}^2$. For this purpose, we will compare the evolved model with JR09 in the range

$$0.015 < x < 0.04. \tag{30}$$

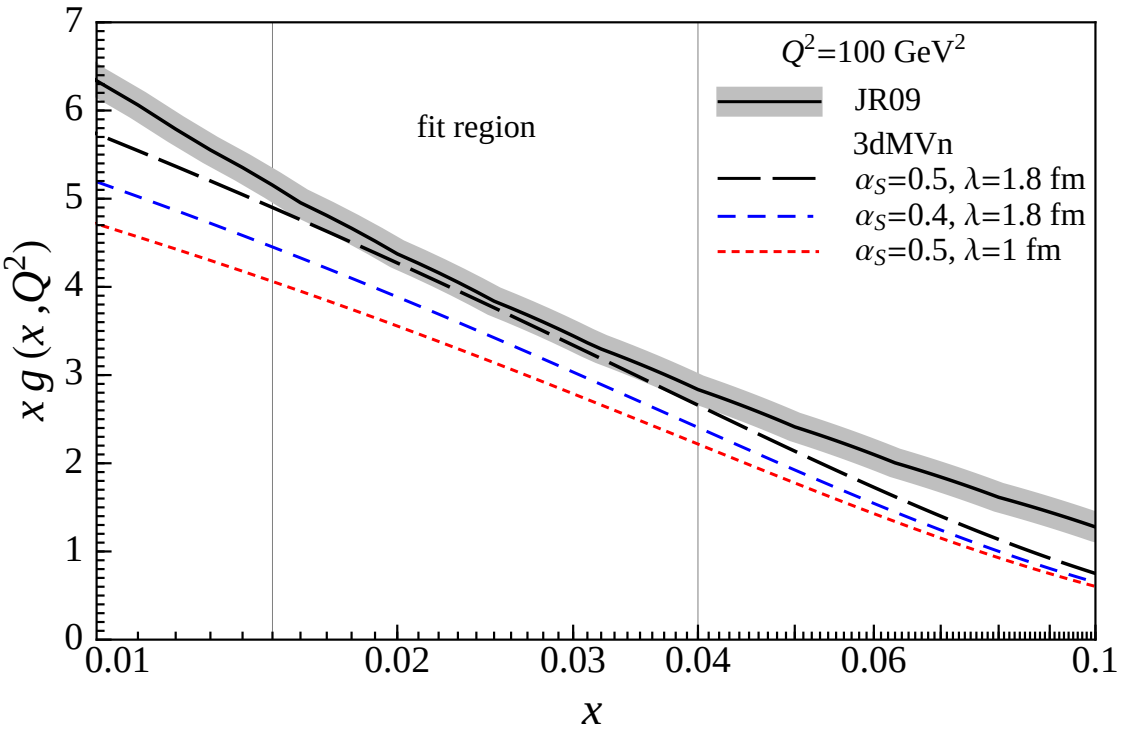


FIG. 2. Comparison of the gluon distribution function of a nucleon from the 3dMVn model for various values of $\{\alpha_s, \lambda\}$ with the JR09 data parametrization at $Q^2 = 100\,\mathrm{GeV}^2$. The horizontal axis is in logarithmic scale. For distances larger than the correlation length $\lambda$, gluons are not correlated and hence the color neutrality condition is satisfied. The model is reliable in the fit region bounded by the two vertical lines. The uncertainty in JR09 is shown with an error band and it is about 5%. The discrepancy between the best fit curve ($\alpha_s = 0.5$ and $\lambda = 1.8\,\mathrm{fm}$) and the JR09 in the fit region is only 2%.

The gluons from $x < 0.015$ do not enter the DGLAP evolution and hence they do not contribute to the region in Eq. (30). The gluons from $0.015 < x < 1$ will enter the DGLAP evolution. We argue that the parametrization in Eq. (27) is a good approximation for the large-x gluons.

Our analysis shows that the best fit occurs at the values $\alpha_s = 0.5$ and $\lambda = 1.8\,\mathrm{fm}$. In Figure 2 we show a comparison between the JR09 data parametrization and 3dMVn model at $Q^2 = 100\,\mathrm{GeV}^2$ for $\alpha_s = 0.5$ and $\lambda = 1.8\,\mathrm{fm}$. We find almost identical plots at other $Q^2$ values in the range $0.015 < x < 0.04$.

At other values of $\alpha_s$ and $\lambda$, we find that the model underestimates the data. As $\alpha_s$ increases, the 3dMVn curve increases and the disagreement between the model and JR09

decreases. For values $\alpha_s \geq 0.5$ the model does not change significantly. Hence, we take $\alpha_s = 0.5$ since this is the smallest value of $\alpha_s$ for which a good fit can be obtained. Interestingly, this "freezing" behavior of the strong coupling constant particularly at $\alpha_s = 0.5$, imposed in other approaches by hand (see [19, 20]), arises naturally in the 3dMVn model. Adjusting $\lambda$ changes the model curve only slightly. For $\alpha_s = 0.4$ and values of $\lambda$ greater than 1.8 fm, we do not find a fit as good as the one for $\alpha_s = 0.5$ and $\lambda = 1.8$ fm.

There are various sources of uncertainty in the MV model which are shared with the 3dMVn model. In the paradigm of strong classical color fields, one wishes to employ solutions of the classical Yang-Mills equation which is given in covariant gauge by

$$(\boldsymbol{\nabla}_\perp^2 + \partial_\parallel^2)A^\nu = gJ^\nu + 2ig[A^\mu, \partial_\mu A^\nu] - ig[A_\mu, \partial^\nu A^\mu] + g^2[A_\mu, [A^\mu, A^\nu]], \tag{31}$$

where $\partial_\parallel^2 = -2\partial_+\partial_-$. The second and third terms on the right hand side of the Eq. (31) are responsible for the three gluon interaction vertex, and the last term is for the four gluon interaction vertex in the quantized theory. In the framework of Color Glass Condensate, only the linearized version of Eq. (31) is used. The nonabelian feature of the model sets in when the solutions of the linearized equation in the covariant gauge are transformed to the light-cone gauge by means of the full gauge transformation including the nonabelian term [7]

$$A^\mu_{\rm LC}(x) = {\rm U}(x)A^\mu_{\rm cov}{\rm U}^{-1}(x) - \frac{i}{g}[\partial^\mu {\rm U}(x)]{\rm U}^{-1}(x). \tag{32}$$

The reason why the nonlinear terms in Eq. (31) are omitted is simply because the solutions of the fully nonlinear theory are not known. In addition, the Green's function for gluons, which is essential in the calculation of $\langle A_i^a(\boldsymbol{x})A_i^b(\boldsymbol{x}\,')\rangle$ from $\langle \rho^a(\boldsymbol{x})\rho^b(\boldsymbol{x}\,')\rangle$, can only be defined in the linear theory. The gluon propagator is calculated from

$$(\boldsymbol{\nabla}_\perp^2 + \partial_\parallel^2)G(\boldsymbol{x}) = \delta^3(\boldsymbol{x}). \tag{33}$$

The origin of the infrared divergences in the MV model lies here and this is also why confinement effects need to be introduced by hand by using colored noise. In principle, the correlation function with colored noise in Eq. (4) should be calculable from the fully nonlinear theory.

The linear approximation can only be justified if $g \ll 1$ so that the nonlinear terms can be neglected. However, the strong coupling constant is not expected to be so small and

nonlinear terms are as important as the source term. Hence, the linear approximation of Eq. (31) is the main source of the uncertainty in any realistic analysis.

Another source of uncertainty may be the assumption that the nucleus is taken to be much larger than a nucleon, $R \gg R_0$. For a gold nucleus, the corrections may be as large as 17% since $R_0/R \sim A^{-1/3} \sim 0.17$. Also quantum corrections at smaller values of x may be important even in the weak coupling limit. These corrections are of the form $\alpha_s \ln(1/x)$ and discussed in the references [5, 6, 8]. Lastly, although we estimate that the error due to neglecting the nuclear effects should be small, it would be worth of repeating the analysis presented in this paper by using nuclear pdf's once they are available for $Q^2 \sim 0.55\,\mathrm{GeV}^2$.

## VII. SUMMARY AND OUTLOOK

The framework of Color Glass Condensate allows one to calculate the vector field correlation function. It can be used to calculate the gluon distribution function of the ultra-relativistic nuclei and the initial energy density distribution due to the interacting classical color fields produced by the colliding nuclei in heavy ion collisions.

We have examined a three dimensional color neutral version of the McLerran-Venugopalan model. The 3dMVn model is finite in the infrared and therefore an infrared cutoff is not needed. In addition, the results of this model are x dependent due to the intrinsic three dimensional treatment of the nucleus in contrast to the approximation of infinitely thin nucleus.

In order to explore the parameter space of these two variables, we have calculated the gluon distribution function for several values of $\alpha_s$ and $\lambda$. The originality of this work is to compare our calculations directly with parametrization of the data to determine the free parameters of the model. We have found the best fit between the gluon distribution function from the JR09 parametrization and the one calculated from the 3dMVn model occurs at $\alpha_s = 0.5$ and $\lambda = 1.8\,\mathrm{fm}$. At other values of these two parameters the model underestimates the data. This may be due to the uncertainty in the assumptions and rough estimates made during the construction of the model as well as the other uncertainties discussed in the previous section. We have also found that the 3dMVn model had an intrinsic freezing behavior that the gluon distribution function froze at $\alpha_s = 0.5$ and remained unchanged for $\alpha_s > 0.5$.

The assumption that the color charge is normally distributed throughout the nucleus lies at the heart of the MV and 3dMVn models. Besides the normal (Gaussian) distribution of the color charge, the nucleonic inner structure of the nucleus is implemented via colored noise by introducing correlations for distances smaller than a nucleon size. In this manner, the fluctuations in the positions of nucleons in a nucleus have not been treated separately from the dynamical color charge fluctuations. In other words, the effect of confinement is realized through short range correlations in $\langle \rho^a(\boldsymbol{x})\rho^b(\boldsymbol{x}')\rangle$ by colored noise rather than considering the nucleus as a collection of individual nucleons. An alternative to this might be an event-by-event Monte Carlo sampling of the distribution of nucleons [21–24]. For a finite nucleus, the results from event-by-event fluctuations in positions of the sampled nucleons may differ from the analytical calculations presented in this paper. For a very large nucleus, we expect the results from both approaches to agree.

The final product of this work is the unintegrated gluon distribution (also known as the "gluon number density") given in Eq. (15) of which parameters are fixed in the previous section. This three dimensional quantity is the main ingredient for various applications of the CGC concept. It can be picked up by the practitioners of CGC and be used immediately in realistic calculations other than calculation of the gluon distribution function.

In this work, we calculated the gluon distribution function since it was a quantity that could be easily compared with data. However, the ultimate goal was not calculating the gluon distribution function per se, but to attain a working model for further use, particularly in the calculation of the initial energy density distribution in heavy ion collisions. This work is in progress. In the future work, we plan to calculate the initial energy density in heavy ion collision in the framework of the 3dMVn model.

## ACKNOWLEDGMENTS

We thank Joseph Kapusta and Rainer J. Fries for useful discussions and their critical comments on the manuscript. We also thank Michiel Botje for correspondence regarding his QCDNUM code. This work was supported by the U.S. DOE Grant No. DE-FG02-

87ER40328.

---


[1] E. Iancu and R. Venugopalan, In *Hwa, R.C. (ed.) et al.: Quark Gluon Plasma* , 249 (2003), arXiv:hep-ph/0303204 [hep-ph].

[2] L. D. McLerran and R. Venugopalan, Phys.Rev. **D49**, 2233 (1994), arXiv:hep-ph/9309289 [hep-ph].

[3] L. D. McLerran and R. Venugopalan, Phys.Rev. **D49**, 3352 (1994), arXiv:hep-ph/9311205 [hep-ph].

[4] L. D. McLerran and R. Venugopalan, Phys.Rev. **D50**, 2225 (1994), arXiv:hep-ph/9402335 [hep-ph].

[5] A. Ayala, J. Jalilian-Marian, L. D. McLerran, and R. Venugopalan, Phys.Rev. **D52**, 2935 (1995), arXiv:hep-ph/9501324 [hep-ph].

[6] A. Ayala, J. Jalilian-Marian, L. D. McLerran, and R. Venugopalan, Phys.Rev. **D53**, 458 (1996), arXiv:hep-ph/9508302 [hep-ph].

[7] C. Lam and G. Mahlon, Phys.Rev. **D61**, 014005 (2000), arXiv:hep-ph/9907281 [hep-ph].

[8] C. Lam and G. Mahlon, Phys.Rev. **D62**, 114023 (2000), arXiv:hep-ph/0007133 [hep-ph].

[9] J. Jalilian-Marian, A. Kovner, L. D. McLerran, and H. Weigert, Phys.Rev. **D55**, 5414 (1997), arXiv:hep-ph/9606337 [hep-ph].

[10] Y. V. Kovchegov, Phys.Rev. **D54**, 5463 (1996), arXiv:hep-ph/9605446 [hep-ph].

[11] V. Gribov and L. Lipatov, Sov.J.Nucl.Phys. **15**, 438 (1972).

[12] L. Lipatov, Sov.J.Nucl.Phys. **20**, 94 (1975).

[13] Y. L. Dokshitzer, Sov.Phys.JETP **46**, 641 (1977).

[14] G. Altarelli and G. Parisi, Nucl.Phys. **B126**, 298 (1977).

[15] M. Botje, Comput.Phys.Commun. **182**, 490 (2011), arXiv:1005.1481 [hep-ph].

[16] J. Jalilian-Marian and X.-N. Wang, Phys.Rev. **D60**, 054016 (1999), arXiv:hep-ph/9902411 [hep-ph].

[17] P. Jimenez-Delgado and E. Reya, Phys.Rev. **D80**, 114011 (2009), arXiv:0909.1711 [hep-ph].

[18] I. Schienbein, J. Yu, K. Kovarik, C. Keppel, J. Morfin, *et al.*, Phys.Rev. **D80**, 094004 (2009), arXiv:0907.2357 [hep-ph].

[19] A. Dumitru, D. E. Kharzeev, E. M. Levin, and Y. Nara, Phys.Rev. **C85**, 044920 (2012), arXiv:1111.3031 [hep-ph].

[20] J. L. Albacete, A. Dumitru, H. Fujii, and Y. Nara, (2012), arXiv:1209.2001 [hep-ph].

[21] B. Schenke, S. Jeon, and C. Gale, Phys.Rev.Lett. **106**, 042301 (2011), arXiv:1009.3244 [hep-ph].

[22] B. Schenke, S. Jeon, and C. Gale, Phys.Lett. **B702**, 59 (2011), arXiv:1102.0575 [hep-ph].

[23] B. Schenke, P. Tribedy, and R. Venugopalan, Phys.Rev.Lett. **108**, 252301 (2012), arXiv:1202.6646 [nucl-th].

[24] B. Schenke, P. Tribedy, and R. Venugopalan, Phys.Rev. **C86**, 034908 (2012), arXiv:1206.6805 [hep-ph].